BIOCHEMISTRY
including biophysical chemistry & molecular biology

Article

pubs.acs.org/biochemistry

The Structure of Human DNase I Bound to Magnesium and Phosphate Ions Points to a Catalytic Mechanism Common to Members of the DNase I-like Superfamily

Goetz Parsiegla,*[,†] Christophe Noguere,[†] Lydia Santell,[‡] Robert A. Lazarus,*[,‡] and Yves Bourne[†]

[†]Architecture et Fonction des Macromolécules Biologiques, Aix-Marseille Université and CNRS UMR 7257, Parc Scientifique et Technonlogique de Luminy, Case 932, 163 Avenue de Luminy, 13288 Marseille cedex 09, France

[‡]Department of Early Discovery Biochemistry, Genentech, Inc., 1 DNA Way, South San Francisco, California 94080, United States

Supporting Information

ABSTRACT: Recombinant human DNase I (Pulmozyme, dornase alfa) is used for the treatment of cystic fibrosis where it improves lung function and reduces the number of exacerbations. The physiological mechanism of action is thought to involve the reduction of the viscoelasticity of cystic fibrosis sputum by hydrolyzing high concentrations of DNA into low-molecular mass fragments. Here we describe the 1.95 Å resolution crystal structure of recombinant human DNase I (rhDNase I) in complex with magnesium and phosphate ions, both bound in the active site. Complementary mutagenesis data of rhDNase I coupled to a comprehensive structural analysis of the DNase I-like superfamily argue for the key catalytic role of Asn7, which is invariant among mammalian DNase I enzymes and members of this superfamily, through stabilization of the magnesium ion coordination sphere. Overall, our combined structural and mutagenesis data suggest the occurrence of a magnesium-assisted pentavalent phosphate transition state in human DNase I during catalysis, where Asp168 may play a key role as a general catalytic base.

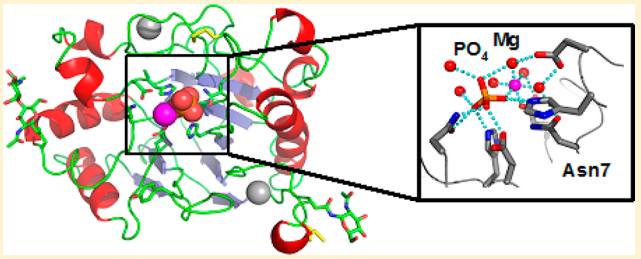

Human deoxyribonucleases (DNases) comprise a family of enzymes that cleave phosphodiester bonds in DNA.[1,2] While these enzymes represent a relatively small subset of all nucleases found in nature,[3,4] they are important for understanding human biology, including nutritional DNA digestion and apoptosis, and one member in particular has had a major therapeutic impact. Indeed, recombinant human DNase I (rhDNase I, Pulmozyme, dornase alfa) is used clinically in the treatment of pulmonary disease in patients with cystic fibrosis (CF).[5−7] In vitro studies have shown that rhDNase I reduces the viscoelasticity of CF sputum because of its capacity to degrade double-stranded DNA into lower-molecular mass fragments.[8] Inhalation of DNase I into the airways improves lung function and reduces the risk of infectious exacerbations.[6,9] rhDNase I treatment has been studied with a variety of other diseases in which extracellular DNA has been postulated to play a pathological role, including systemic lupus erythematosus (SLE),[10,11] mechanical ventilation,[12] atelectasis,[13] chronic sinusitis,[14] and empyema.[15,16] It is interesting to note that G-actin binds DNase I with high affinity and is a potent inhibitor (K_i = 1 nM) of DNA hydrolytic activity in CF sputum and thus may potentially influence the effectiveness of DNase I in vivo.[17,18]

DNase I hydrolyzes double-stranded DNA nonspecifically between the 3′-oxygen atom and the phosphorus to yield 3′-hydroxyl and 5′-phosphoryl nucleotides using a single-strand nicking mechanism.[19] From a biochemical and structural perspective, pancreatic bovine DNase I (bDNase I) has been the most widely studied endonuclease in this family.[62,21] Several studies have demonstrated the critical role of divalent metal ions in the catalytic activity of DNase I, with the requirement for Ca^{2+} as well as a strong dependence on other divalent cations such as Mg^{2+} and Mn^{2+}.[22−24] Increased levels of Mg^{2+} are found in the CF sputum of clinical responders treated with rhDNase I, and adding Mg^{2+} to rhDNase I reduces the viscosity of CF sputum ex vivo.[25]

Crystal structures of bDNase I have been determined alone and in complex with cleaved or uncleaved DNA, leading to a relatively comprehensive view of DNA binding in the active site. Overall, these structures emphasize DNA deformation during the catalytic process[26−29] and have been valuable in providing the molecular basis for engineering human DNase I variants that are resistant to inhibition by G-actin,[30] as well as those having increased catalytic activity.[31,32] Recent structural studies of more distantly related members of the DNase I-like superfamily in complex with cations or DNA, e.g., the apurinic/apyrimidinic endonucleases from human (hAPE1) and *Neisseria meningitidis* (Nape), the sphingomyelin phosphodiesterase (SMase) from *Bacillus cereus*, or the C-terminal domain of

Received: June 29, 2012
Revised: December 7, 2012
Published: December 7, 2012

human CNOT6L nuclease (hCNOT6L), have led to proposed catalytic mechanisms for either hAPE1 and hCNOT6L or SMase.[33−37] An extensive iterative sequence comparison based on these members of the DNase I-like superfamily suggests the existence of a conserved pattern of functional amino acids that conduct various functions by means of a common catalytic mechanism.[34] However, the crystal structure of a mammalian DNase I with a bound divalent metal ion in the active site, which is crucial for understanding its catalytic mechanism, has remained elusive.

Here we report the 1.95 Å resolution crystal structure of rhDNase I in complex with divalent cations and phosphate. Two Ca^{2+} ions are located at each extremity of the active site, and a Mg^{2+} and the phosphate ion are bound in its center. We also reveal the unprecedented critical catalytic role of rhDNase I Asn7, a residue that is invariant among mammalian DNase I enzymes and members of the DNase I-like superfamily. Superposition of the active site of rhDNase I with those from bDNase I and other members of the DNase I-like structural superfamily determined in complex with DNA and divalent metal ions allows us to propose a novel transition state of human DNase I during the Mg^{2+}-assisted cleavage mechanism.

MATERIALS AND METHODS

Expression, Purification, and Crystallization. Recombinant fully active human DNase I (rhDNase I) was produced by genetically engineered Chinese hamster ovary (CHO) cells containing DNA encoding the native human protein. rhDNase I was purified by tangential flow filtration and liquid chromatography. Purified rhDNase I used for crystallization contains 260 amino acids with an approximate molecular mass of 37000 Da and no His_9 tag (see below). The primary amino acid sequence is identical to that of the native human enzyme. Initial crystals of rhDNase I were obtained by the sitting drop vapor diffusion technique using the JCSG+ (Molecular Dimensions) screening kit at 18 °C, using a pure solution of the rhDNase I at a concentration of 10.5 mg/mL in 0.02 M sodium phosphate buffer (pH 7.0). Crystallization assays were performed using droplets of 200 nL as previously described.[38] Small crystals grew in droplets containing equal amounts of the protein solution and buffer [0.2 M $MgCl_2$, 0.1 M Bis-Tris (pH 5.5), and 25% PEG 3350]. Crystals suitable for X-ray diffraction studies under cryo-conditions were obtained manually using macro-seeding techniques and hanging drop vapor diffusion under the same conditions.

rhDNase I and Asn7 Mutants. rhDNase I mutants containing an Ala or a Ser substitution at position 7 were made by mutagenesis using QuikChange II XL site-directed mutagenesis (Agilent), and the correct mutations were verified by DNA sequencing. A His_9 tag was also introduced into all constructs at the C-terminus to facilitate purification. Wild-type rhDNase I, Asn7Ala, and Asn7Ser were expressed in CHO cells by transient transfection and purified sequentially by Ni-NTA (Qiagen, Valencia, CA) and size exclusion {Superdex 75 10/300 GL [20 mM HEPES (pH 7.2) and 150 mM NaCl], GE Healthcare, Piscataway, NJ} chromatography steps. Fractions containing eluted proteins were analyzed by sodium dodecyl sulfate−polyacrylamide gel electrophoresis (SDS−PAGE) (4 to 20%) and pooled. Protein concentrations were determined by a DNase I enzyme-linked immunosorbent assay and absorbance at 280 nm.[30−32] Wild-type rhDNase I and Asn7 mutants were characterized for activity using the linear plasmid digestion and hyperchromicity activity assays essentially as previously described.[30−32] The linear plasmid digestion assay used 10 ng/mL rhDNase I in 25 mM HEPES (pH 7.0), 100 μg/mL BSA, 1 mM $MgCl_2$, 2.5 mM $CaCl_2$, and 150 mM NaCl, and the hyperchromicity assay used 1 μg/mL rhDNase I in 25 mM HEPES (pH 7.0), 4 mM $MgCl_2$, 4 mM $CaCl_2$, and 150 mM NaCl. For comparison, clinical grade Pulmozyme, which lacks the His_9 tag, was also included as a control in the assays. Proper folding of these mutants was determined using one-dimensional (1D) nuclear magnetic resonance (NMR) (Figure S1 of the Supporting Information) and was consistent with their behavior during purification and when detected using antibodies directed against rhDNase I (data not shown).

Data Collection and Phasing. Data sets were collected at ESRF beamline ID23-1 (Grenoble, France) under cryo conditions at a wavelength of 0.98 Å using an ADSC Q315 detector. Data processing with the XDS package indicated the crystal belongs to space group $P2_12_12_1$.[39] After reflection data had been scaled using XSCALE, a 99.7% complete data set up to 1.95 Å resolution was assembled; 5% of the experimental data was set aside for the calculation of R_{free}.[40] Initial phases were obtained by molecular replacement with MOLREP from CCP4 program suite version 6.0.2[41,42] using coordinates of native bovine DNase I [chain A, Protein Data Bank (PDB) entry 3DNI] as the starting model. The molecular replacement search produced a single unambiguous result with R_{factor} and R_{free} of 0.435 and 0.448, respectively.

Refinement. Structural refinement was performed using Refmac from the CCP4 package.[42] All manual model construction and sequence exchange with rhDNase I were performed with COOT version 0.3.3.[43] The difference density maps obtained from an initial rigid body refinement after sequence replacement showed that significant changes were limited to Tyr73 and the Cys101−Asn106 surface loop containing a disulfide bridge and a glycosylation site. We were able to fit two GlcNAc residues at the Asn18 glycosylation site and one GlcNAc residue at Asn106. Difference peaks in the active site of rhDNase I corresponded to two Ca^{2+} ions also present in bDNase I or were interpreted as being caused by their coordination sphere and the shape of their electron density as a magnesium ion sharing a coordinating atom with a phosphate ion. A calculated difference Fourier map using the anomalous signal at 0.98 Å showed a reasonably intense peak for one of the two calcium atoms but no signal for the magnesium atom, consistent with absorption edges. An additional difference density in the vicinity of the magnesium ion was interpreted as a Bis-Tris molecule arising from the crystallization buffer, sandwiched between Trp187 and Pro190 at the packing interface. The Bis-Tris molecule establishes a direct hydrogen bond with the main chain carbonyl of Thr188 and an H-bond with another water molecule from the coordination sphere of the Mg^{2+} ion from the symmetry-related molecule. Finally, water molecules were added first using the automated function in COOT and later manually refined. Data collection and refinement statistics are listed in Table 1. Structural homologues were detected using DaliLite server version 3.0 and the SCOP database.[44,45] All figures and structural pairwise overlays (Table S2 of the Supporting Information) were made using PyMOL.[46] Coordinates and structure factors were deposited in Protein Data Bank (entry 4AWN).

Table 1. Data Collection and Refinement Statistics[a]

	rhDNase I·$H_xPO_4^{y-}$·$MgCl_2$[b]
resolution (Å)	50−1.95
unit cell [*a*, *b*, *c* (Å)]	41.96, 58.66, 96.43
space group	$P2_12_12_1$
completeness (%)	99.7 (99.0)
multiplicity	7.1 (7.2)
$I/\sigma I$	7.6 (1.6)
R_{merge} (%)	9.3 (49.0)
no. of unique reflections	17963
no. of protein atoms	2109
no. of water molecules	208
average *B* factor for protein (Å^2)	23.8
average *B* factor for Mg^{2+}, $H_xPO_4^{y-}$ ion, water (Å^2)	24.6, 22.3, 32.5
R, R_{free} (%)	16.6 (20), 21.9 (29)
rmsd for bond lengths (Å)	0.013
rmsd for bond angles (deg)	1.43
rmsd for dihedral angles (deg)	0.102
Ramachandran plot (%) (most favored, allowed, outlier)	98.4, 1.6, 0

[a]Values in parentheses correspond to those of the highest-resolution shell. [b]For $H_xPO_4^{y-}$, the anion may be a hydrogen ($x = 1$; $y = 2$) or dihydrogen ($x = 2$; $y = 1$) phosphate.

RESULTS

The final structure of rhDNase I encompasses the mature protein from Leu1 to Lys260 and is folded into a four-layer α/β sandwich, which is an architecture typically found for all members of the DNase I-like structural superfamily (Figure 1A). Its closest structural homologue is bDNase I (PDB entry 3DNI), with a sequence that is 78% identical and rmsds of 0.71 Å and 0.66 Å for all main chain and Cα atoms, respectively (Figure S3 of the Supporting Information). Here we present novel structural features found in rhDNase I; for a comprehensive view of the closely related bDNase I, see reviews by Suck[47] and Chen and Liao.[20]

The structure of rhDNase I contains two N-linked glycan chains attached to two Asn residues conserved in bDNase I at positions 18 and 106 (rhDNase I numbering is used for the description of structurally conserved residues throughout). Two structural Ca^{2+} ions are located in cation binding sites close to Asp201 (site I) and Asp107 (site II), both flanking the active site cleft as already identified in bDNase I structures.[48] Although glycosylation at the first site is also observed in bDNase I, glycosylation at the latter one has not been described yet, although it has been found in ternary structures of bDNase I in complex with actin and other actin-binding proteins involved in Wiskott-Aldrich syndrome.[49] In rhDNase I, Asn106 is located in a partly disordered surface loop next to Ca^{2+} site II and adopts an orientation different from that observed in the ternary complexes with proteins involved in Wiskott-Aldrich syndrome, where this Ca^{2+} site is absent. Like bDNase I, the human enzyme contains the same two disulfide bridges, i.e., Cys101−Cys104 and Cys173−Cys209. The first disulfide bridge, located in the same short surface loop that encompasses the glycosylation site at Asn106, is broken, resulting in an inter-sulfur distance of 3.06 Å, most likely caused by radiation damage during data acquisition. However, even though the disulfide bond is broken, the ion binding site in the proximity is occupied with a Ca^{2+} ion in an appropriate manner, providing evidence that the local structure is unaffected. The second

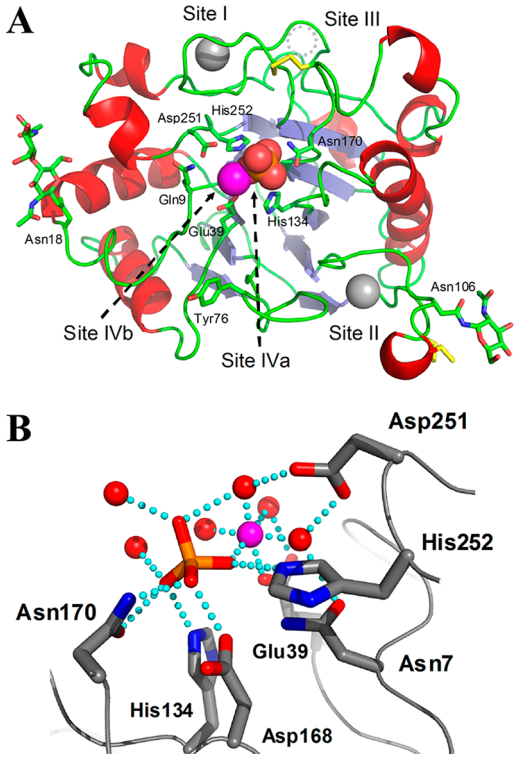

Figure 1. (A) Overall fold of rhDNase I. Three ion binding sites (labeled I, II, and IV) are occupied by two Ca^{2+} ions (gray), a Mg^{2+} (magenta), and a phosphate (orange/red). N-Linked glycosylation sites at positions Asn18 and Asn106 as well as the coordinating side chains at site IV and the orientations of side chains Gln9 and Tyr76 are indicated. The two disulfide bridges (the 101−104 bridge is broken) are colored yellow. (B) Close-up view of site IV and the rhDNase I magnesium phosphate complex. The Mg^{2+} ion is colored magenta. Its primary, hexagonal bipyramidal coordination sphere and the coordination of water molecules involved in the primary coordination sphere are shown. All direct interactions of the tetrahedral phosphate ion (orange) and H-bonds are indicated.

Cys173−Cys209 disulfide is well-defined and adopts a geometry similar to that found in bDNase I.

Active Site. Upon comparison of the DNA binding region of bDNase I bound to DNA[26,28] with the corresponding region of rhDNase I, two important differences are noticeable. The first concerns the arc motion of the Tyr76 side chain, one of the key residues involved in DNA binding in bDNase I.[50] Indeed, this aromatic residue induces a distortion of the DNA backbone conformation to precisely position the scissile phosphodiester bond into the active site. This Tyr residue is important for DNA hydrolysis in both the human and bovine enzymes, as demonstrated by the almost total loss of activity with the corresponding Ala mutant.[32,50] In the rhDNase I structure, Tyr76 swings outside the active site into the solvent and adopts an unusual *cis* peptide bond with the adjacent Ser75 residue. While the new orientation of the Tyr phenol ring is stabilized by crystal packing interactions, the observed motion of this side chain is consistent with a certain flexibility of this side chain in solution, as previously shown in the bovine apoenzyme and in its complex with actin,[51] in contrast to a more rigid character upon binding to DNA.[26,27] The second difference concerns the nonconserved Gln9 residue in rhDNase I that is replaced by an Arg in bDNase I and other residues in DNase I-related enzymes. Possible effects of this substitution for either

stabilization of the divalent ion in the active site or DNA affinity are discussed below.

In addition to the conformational adaptations observed in the human enzyme, the most striking new feature in rhDNase I is the presence of an ordered Mg^{2+} ion and a phosphate ion both bound to the active site within site IV (Figure 1B). The Mg^{2+} ion is located in the proximity of the proposed DNA cleavage site, which is occupied by the phosphate ion. Although divalent metal ions are essential for DNase I catalysis,[24] no structure of a mammalian DNase I containing a divalent ion in the active site has been reported to date. Our study reveals a characteristic octahedral coordination sphere for the bound Mg^{2+} ion, in which a single carboxylate oxygen of Glu39 forms a direct interaction with the metal ion. Previous modeling studies of the catalytic DNA complex of human DNase I using DNA complexes of bDNase I with an unpublished structure from human DNase I[52] as a template led to the proposal that Glu39, Asp168, and Asp251 participate in Mg^{2+} ion coordination.[32] Notably, Asp168 does not participate in the coordination sphere of the Mg^{2+} ion as proposed initially. Instead, it interacts directly with the phosphate ion as do His252, His134, and Asn170. The remaining ligands of the bipyramidal coordination sphere of Mg^{2+} are one oxygen from the phosphate ion, two water molecules bound to either Asp251 or Asn7, a third water molecule bound to the second carboxylate oxygen of Glu39, and a fourth solvent-exposed water molecule (Figure 1B). The Mg−O distances range from 1.95 to 2.25 Å, which are typical for magnesium coordination sites in proteins.[53]

DNase I Mutagenesis. Previous studies have elucidated the effect of substitution of key residues in the active site for both rhDNase I[30,32] and bDNase I.[54] In rhDNase I, alanine substitution at 15 critical positions within or close to the catalytic site resulted in either a total or a very significant loss of activity: Gln9, Glu39, Arg41, Asn74, Tyr76, Glu78, Arg111, His134, Asp168, Asn170, Tyr175, Arg211, Asp212, Asp251, and His252. Similar reductions in catalytic activity were observed in bDNase I at positions Arg9, Arg41, Tyr76, Glu78, His134, Asp168, Asp212, and His252, albeit using different substitutions in some instances.[54] Residues involved in the coordination of the Ca^{2+} cations at sites I and II have been mutated for both rhDNase I[55] and bDNase I,[56,57] again with similar results for the two enzymes. Furthermore, residues contacting the phosphate backbone have been investigated by mutational analysis in both rhDNase I[32] and bDNase I,[56] defining a common set of interactions for the two enzymes. To further investigate the functional role of the second-sphere active site residues, we characterized two novel mutants to evaluate the implication of Asn7 in the catalytic mechanism of rhDNase I. Asn7Ser and Asn7Ala variants as well as the wild type were expressed and purified to homogeneity; the expression level of all three proteins was similar (Figure S4 of the Supporting Information). We could not detect any catalytic activity for either of the Asn7 mutants using either linear plasmid digestion or hyperchromicity assays (Figure 2). On the basis of standard curves using the more sensitive hyperchromicity assay (data not shown), the Asn7 mutants have <0.1% of the activity of the wild-type enzyme. To ensure that the Asn7 mutants were folded proteins, we conducted 1D NMR experiments. Here we observed characteristic peaks for protein resonances that are nearly identical in spectra for wild-type and Asn7 mutant proteins (Figure S1 of the Supporting Information); in particular, the patterns of peaks upfield of 0 ppm are indicative of structured correctly folded proteins. Because the protein fold of these mutants is intact, we conclude that Asn7 plays a critical role in the catalytic mechanism. As observed in the crystal structure of rhDNaseI, Asn7 participates indirectly in the coordination sphere of the Mg^{2+} ion with an H-bond of its amide oxygen with a coordinated water molecule and connects Asp168 and Glu39 with an H-bonding network via its amide nitrogen (Figure S5 of the Supporting Information). In fact, Asn7 is invariant among 10 mammalian DNase I enzymes and in the three human DNase I-like enzymes (Table S6 of the Supporting Information). Furthermore, Asn is also found at this structural position in all members of the DNase I-like superfamily, including human and bacterial APE enzymes, SMase, and hCNOT6L (Table S2 of the Supporting Information). Furthermore, a similar mutation in hCNOT6L resulted in a loss of enzymatic activity, supporting the importance of an Asn at position 7 in all nucleases of this superfamily.[37]

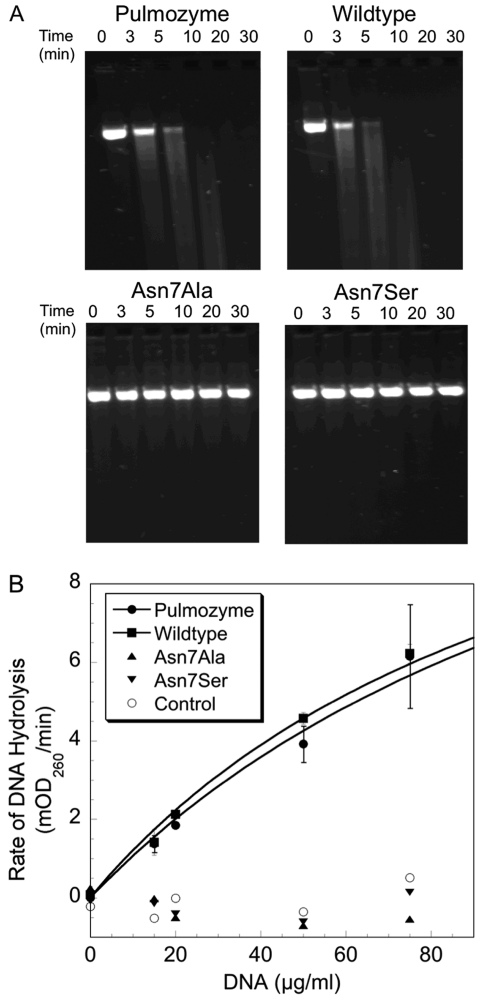

Figure 2. Catalytic activity of human DNase I and Asn7 mutants. The activity of rhDNase I and the Asn7Ala and Asn7Ser mutants was measured using two independent assays. All proteins except Pulmozyme contain a C-terminal His_9 tag. (A) Degradation of linearized plasmid DNA in the presence of rhDNase I or the Asn7 mutants as a function of time (minutes). (B) Hyperchromicity assay data that show the increase in the initial rates of DNA hydrolysis (ΔA_{260} per minute) vs DNA concentration in the presence or absence of 1 μg/mL rhDNase I, Pulmozyme, or the Asn7 mutants.

DISCUSSION

Crystal structures from other distantly related members of the DNase I-like superfamily, such as hAPE1 (17% identical sequence) and Nape (17% identical sequence), SMase (16% identical sequence), or hCNOT6L (13% identical sequence), contain a Mg^{2+} ion in the active site and can be compared to the binding mode of the Mg^{2+} ion in rhDNase I (Table S7 of the Supporting Information).[45] Comparison of the active site of rhDNase I with those from SMase and hCNOT6L reveals a similar location for the bound Mg^{2+} ion. Residues involved in magnesium and phosphate coordination in rhDNase I are structurally conserved in these two structures as well as in bDNase I. The rmsd values in the C_α positions of these coordinating residues between hCNOT6L or SMase and rhDNase I are very small, ranging from 0.42 to 0.47 Å (Asn7, Glu39, His134, Asp168, Asn170, Asp251, and His252). Side chains involved in the Mg^{2+} coordination sphere adopt a similar conformation in the SMase·Mg^{2+} complex,[36] even if the phosphate ion is absent from this structure or if a second Mg^{2+} ion or an adenosine monophosphate (AMP) molecule is located in the phosphate ion site as observed for the hCNO6TL complex.[37] Such a structural conservation in the Mg^{2+} coordination sphere among these three DNases belonging to the DNase I-like family argues for a conservation of the Mg^{2+} binding site in bDNase I and rhDNase I.

A recent molecular dynamics simulation study predicted the number and location of cation binding sites in bDNase I.[58] In this work, Guéroult et al. proposed the presence of four cation binding sites that can be deconstructed into two high-affinity sites (I and II) for Ca^{2+} ions and two others (III and IV) with a preference for Mg^{2+} ions (Figure 1A). We use the ion site numbering proposed in their paper throughout. The structures of bDNase I alone and in complex with G-actin have previously shown the presence of Ca^{2+} ions at sites I–III.[29,51] While residues involved in the coordination sphere of sites I and II are conserved in rhDNase I, those at site III show variations with two Asp172Gly and Asn208His nonconservative substitutions. This might explain why only sites I and II are occupied in rhDNase I and no ion could be observed at the corresponding site III. Site IV is located adjacent to the active site and comprises two subsites (IVa and IVb) within ~5 Å of each other, each of them being potentially able to interact with a Mg^{2+} cation. In the molecular dynamics study of bDNase I, the putative Mg^{2+} ion at site IVa is coordinated by Asp168, Asp212, and His252, whereas that at site IVb interacts with Asn7 and Glu39.[58] The structure of rhDNase I reveals that the Mg^{2+} cation occupies only subsite IVb, with a single direct coordination from the Glu39 carboxylate, while a solvent-mediated interaction provides interaction with the amide oxygen of Asn7. Unlike the study with bDNase I, site IVa overlaps with the phosphate binding site in the rhDNase I structure, and we could not find any evidence of a second Mg^{2+} cation bound at this subsite. Nevertheless, the active sites of hCNOT6L and hAPE1 reveal a second cation bound at this subsite pointing toward the unprotonated negatively charged state of Asp168 in these complexes.

In rhDNase I, Gln9 does not participate in the coordination sphere of the Mg^{2+} ion but is located proximal to the metal site. This residue is not strictly conserved in the sequences of DNase I and DNase I-like enzymes, where the nature of the substitution may influence the relative position of ions bound to the site. Gln9 is replaced with arginine, tyrosine, leucine, and aspartate or asparagine in bDNase I, SMase, hCNOT6L, and the distantly related hAPE1 or Nape, respectively. In hAPE1, the structural similarity around the cation binding site with rhDNase I depends also on the type and number of cations present in the active site. In fact, two close but distinct locations of the divalent ions are observed in hAPE1 at site IVb.[34,59,60] If the Asp/Asn corresponding to Gln9 (rhDNase I numbering) in the hAPE and Nape enzymes participates in the cation coordination sphere, as found when only a single Mg^{2+}, Pb^{2+}, or Sm^{3+} ion is bound, these ions are pushed 1–1.8 Å away from the Mg^{2+} position observed in the rhDNase I active site. The situation is different in hAPE1 if a single Mn^{2+} ion and cleaved DNA or if not one but two Pb^{2+} ions are present.[59] In that case, Asp9 does not interact with the divalent ions, which are in turn only slightly displaced from the Mg^{2+}·rhDNase I position. The corresponding Leu and Tyr substitutions in hCNOT6L and SMase do not interact with the ions, and if one or even two Mg^{2+} ions are bound in the active site, one of these ions is always located at the same position as Mg^{2+}·rhDNase I.

In bDNase I, Gln9 is replaced with a bulky and positively charged arginine, which is unlikely to coordinate this divalent cation. In this structure, the Arg9 guanidinium group adopts three distinct orientations that prevent prediction of a precise location in the Mg^{2+}-bound state. This structure of rhDNase I is not consistent with the Arg9–Glu39 polar interaction observed in the structure of bDNase I in complex with a scissile DNA (PDB entry 2DNJ)[26] lacking the divalent ion. Site-directed mutagenesis experiments demonstrated the important role of Gln9 for the interaction with the DNA backbone, as mutation into a positively charged Arg led to an increase in enzymatic activity.[31] Structural comparison with hAPE1 reveals that the observed decrease in rhDNase I activity for the corresponding Asp mutant not only might be due to a charge repulsion effect with the DNA backbone but also might be related to its proximity to the coordination sphere of the divalent ion.

The location of the phosphate ion in the rhDNase I·Mg^{2+} complex is reminiscent of that in the hAPE1 complexes with cleaved and uncleaved apurinic DNA (PDB entries 1DE9 and 1DE8). The 5′-phosphate of the scissile apurinic DNA and the phosphate of the uncleaved apurinic DNA are only 0.5 or 0.3 Å from the phosphate ion position in rhDNase I, respectively (Figure 3). Similarly, the positions of the phosphate backbone of the DNA chain in the bDNase I complex (PDB entry 1DNK) and the 5′-phosphate in the hCNOT6L·AMP complex (PDB entry 3NGN) are shifted by only 0.5 and 0.2 Å, respectively. Notably, all 5′-phosphates in hAPE1 and hCNOT6L and the phosphate ion in rhDNase I are oriented similarly and interact with Asp168, a situation not observed for the differently oriented phosphate bridges in the two complexes of bDNase I and hAPE1 with uncleaved DNA. The apparent direct short (~2.6 Å) H-bond of Asp168 with the negatively charged phosphate ion is due to the protonation state of the phosphate ion, which cannot be directly assessed in the crystal structure. The proton from a HPO_4^{2-} or, somewhat more likely, a $H_2PO_4^-$ ion is capable of forming an H-bond with the carboxyl group. This arrangement is observed in all three complexes and is consistent with the role of Asp168 as the proton acceptor during catalysis.

Implications for the Transition State. Comparative analysis of the structure of rhDNase I with those of bDNase I in the two DNA complexes and hAPE1 in complex with Mn^{2+} and DNA reveals the central and essential role of the divalent ion during catalysis and illustrates the phosphate conformations

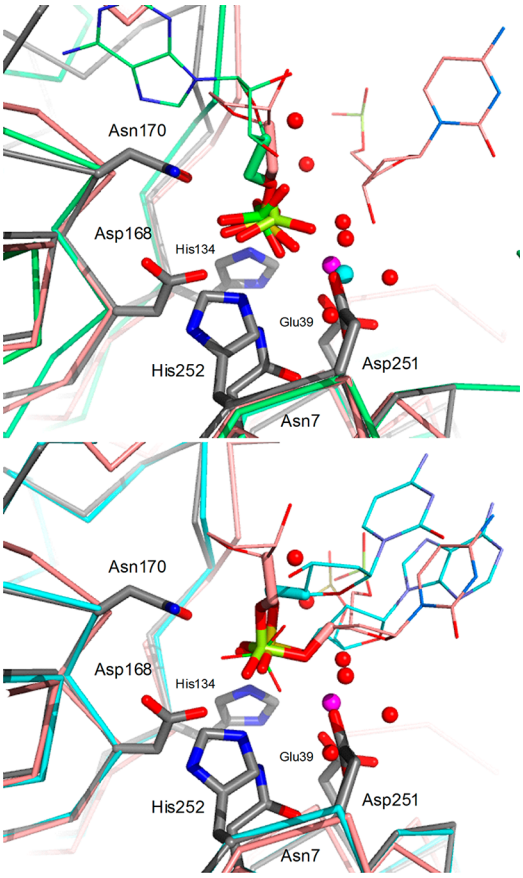

Figure 3. Comparison of rhDNase I with other members of the nuclease superfamily. The top panel shows an overlay of rhDNase I and its primary coordinating residues with carbon atoms colored gray and phosphorus colored green with cleaved DNA from hAPE1 with carbon atoms colored salmon and phosphorus colored lemon (PDB entry 1DE9) and AMP from CNOT6L nuclease with carbon atoms colored light green and phosphorus colored orange (PDB entry 3NGN). Also indicated are the Mn^{2+} ion (cyan) from hAPE1 and the phosphate ion (green), Mg^{2+} ion (magenta), and coordinating water molecules (red) from rhDNase I. The bottom panel shows an overlay of rhDNase I with carbon atoms colored gray with uncleaved DNA from hAPE1 with carbon atoms colored salmon and phosphorus colored lime (PDB entry 1DE8) and bDNase I with carbon atoms colored cyan and phosphorus colored orange (PDB entry 1DNK). The phosphate ion from rhDNase I (with phosphorus colored green) representing the inverted geometry after cleavage shown above is overlaid as thinner lines for comparison.

before and after cleavage (Figure 3). In the bDNase I complex, the position of the phosphate ion is only 0.4 Å from the scissile phosphate in uncleaved DNA and overlays nicely with the 5′-terminal phosphate from cleaved DNA in the hAPE1 complex. The positions of the oxygen atoms in the tetrahedral phosphate ion are rotated by ∼60° compared to those of the 5′-phosphoribose moiety in the uncleaved DNA complexes. This could result from a release of structural restraints in absence of the 5′-bond to the DNA backbone. As found in the hAPE1·DNA complex, the phosphate ion in rhDNase I establishes a direct interaction (2.6 Å) with Asp168 (Asp210 in hAPE1). A simple rotation of 60° of the phosphate toward the 5′-ribose hydroxyl would coincide with the proper phosphate orientation observed in the hAPE1·Mn^{2+}·DNA complex. In this orientation, the geometry of the phosphate ion is inverted compared to that in the bDNase I complex with uncleaved DNA, consistent with an S_N2-like mechanism during catalysis. The striking structural similarity between the hAPE1·Mn^{2+}·DNA complex and the rhDNase I·Mg^{2+}·phosphate complex leads us to propose the occurrence of a pentavalent, trigonal bipyramidal phosphate transition state in rhDNase I, similar to the one proposed for hAPE1[33] (Figure 4). In the catalytic mechanism proposed for bDNase I by Jones

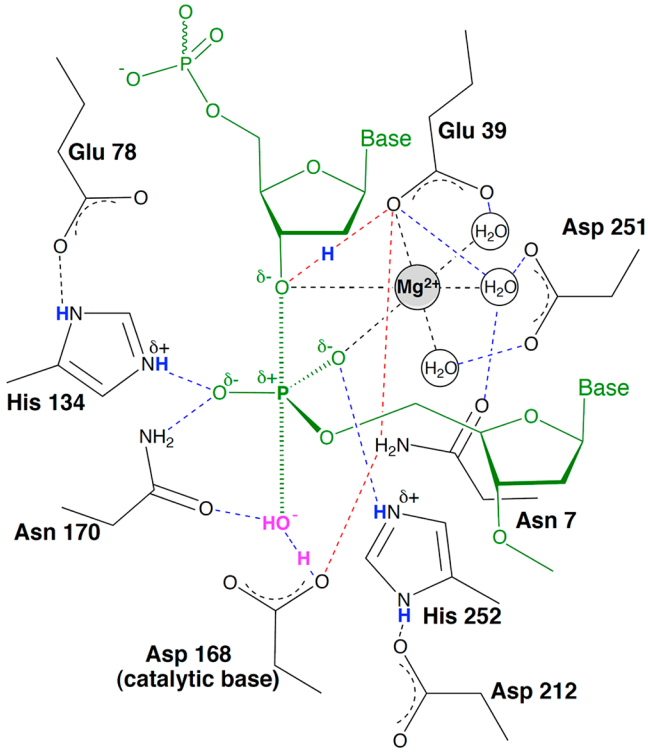

Figure 4. Scheme of a putative transition state during S_N2-like nucleophilic attack. The coordination sphere of the Mg^{2+} ion is colored black and DNA green, and hydrogen bonds are colored blue. To create the intermediate state, His134 could protonate one phosphoryl oxygen of the phosphodiester bond, while His252 stabilizes the other. Asp168 acts as the catalytic general base by deprotonating a water molecule (magenta) that attacks the phosphodiester bond. The H-bonding network connecting Asn7 with the dense hydrogen network around the 3′-ribose oxygen of the pentavalent bipyramidal phosphate transition state (top) and attacking nucleophile (bottom) is colored red.

et al. in which not one but two metal ions participate, Asp168 and His134/Glu78 and His252/Asp212 residue pairs have been proposed as the principle ionizing residues.[54] Here, the latter two would act as the catalytic acid and base, respectively, activating the nucleophile and protonating the ribose 3′-phosphodiester bond. In our model, these two histidine pairs stabilize the planar transition state as previously shown by NMR studies for one His252/Asp212 pair in hAPE1.[61] To induce the pentavalent transition state, "basic" His252 might interact with the acidic phosphoryl oxygen of the phosphate diester, while a protonated "acidic" His134 favors H-bond formation with the negatively charged transition state of the scissile phosphate. This attribution of the hydrogen bonding pattern would be consistent with the pH profiles of these residues in bDNase I determined using chemical rescue,[62] and the structure of SMase in complex with two cobalt ions where His252 participates in the coordination sphere of one of the cations.

In analogy with SMase, where it has been shown that the Lewis acid strength of the divalent ion is critical for catalytic activity,[36] the catalytic Mg^{2+} ion could serve as a Lewis acid to stabilize the reaction intermediate during cleavage of the 3′-phosphoribose bond. Asp168 can act as the catalytic general base in rhDNase I and interact with a water molecule as proposed in hAPE1 and hCNOT6L. Its importance in the catalytic activity of both rhDNase I and bDNase I has been demonstrated previously using site-directed mutagenesis experiments.[32,54] We suggest that the functional role of Asn7 in rhDNase I favors optimal coordination of the bound Mg^{2+} ion, thus generating an appropriate hydrogen bonding network between Asp168 and Glu39. Hence, Asn7 could assist in the transfer of a proton between the attacking water molecule (hydroxide ion) and the ribose during catalysis (the connecting hydrogen bonding network via Asn7 is indicated in Figure 4), which is consistent with our mutagenesis data for this residue (Figure 2).

Conclusions. The novel structure of rhDNase I presented herein reveals the precise location and coordination sphere of the Mg^{2+} ion bound at subsite IVb along with the orientation of key side chains in the active site. Together with a bound phosphate ion, this structure documents the essential role of this divalent ion for catalysis. Structural overlays of rhDNase I with other members of the DNase I-like superfamily in complex with DNA and divalent ions offer new insights into the catalytic mechanism and deepen our understanding of the mutational effects on binding and catalysis. In addition to the previously published structures of the bovine enzyme in the absence or presence of bound DNA,[26−29] this study provides a more reliable template for future modeling or biochemical structure−function studies of human DNase I with DNA.

■ ASSOCIATED CONTENT

Ⓢ Supporting Information

NMR data confirming the correct folding of Asn7 mutants (Figure S1), conservation of active site residues in the DNase I-like superfamily used in pairwise structural overlays with rhDNase I (Table S2), sequence alignment and a structural superposition between rhDNaseI and bDNaseI (Figure S3), interactions of Asn7 in rhDNase I (Figure S4), SDS−PAGE of purified proteins used for activity assays (Figure S5), sequence alignment of key residues in the active site of mature mammalian DNase I and human DNase I-like proteins (Table S6), and selection of members of the DNase I-like superfamily with available structures in the absence or presence of bound ligands (Table S7). This material is available free of charge via the Internet at http://pubs.acs.org.

■ AUTHOR INFORMATION

Corresponding Author

*G.P. (present address): Enzymologie Interfaciale et Physiologie de la Lipolyse, Aix-Marseille Université and CNRS UMR 7282, 31 Chemin Joseph-Aiguier, F-13402 Marseille cedex 20, France; telephone, +33 491 164 192; fax, +33 491 715 857; e-mail, goetz.parsiegla@imm.cnrs.fr. R.A.L.: telephone, 1 650 225 1166; e-mail, lazarus.bob@gene.com.

Author Contributions

Groups of Architecture et Fonction des Macromolécules Biologiques (under Y.B.) and the Department of Early Discovery Biochemistry of Genentech, Inc. (under R.A.L.), contributed equally to this work.

Funding

This work was supported in part by the CNRS and Genentech, Inc.

Notes

L.S. and R.A.L. are employees of Genentech, Inc., which manufactures Pulmozyme.

■ ACKNOWLEDGMENTS

We acknowledge the European Synchrotron Radiation Facility for beam time allocation and thank the ID23-1 staff for assistance during data collection. We also acknowledge Roger Pai for rhDNase I, Blair Wilson and Karen Billeci for analytical biochemistry data and discussions, Till Maurer for 1D NMR experiments, and Laetitia Malphettes and Andy Snowden for helpful discussions.

■ ABBREVIATIONS

DNase, deoxyribonuclease; rhDNase I, recombinant human DNase I; bDNase I, bovine DNase I; CF, cystic fibrosis; hAPE1, apurinic/apyrimidinic endonuclease from human; Nape, apurinic/apyrimidinic endonuclease from *N. meningitidis*; SMase, sphingomyelin phosphodiesterase from *B. cereus*; hCNOT6L, C-terminal domain of human CNOT6L nuclease; CHO, Chinese hamster ovary; rmsd, root-mean-square deviation.

■ REFERENCES

(1) Baranovskii, A. G., Buneva, V. N., and Nevinsky, G. A. (2004) Human deoxyribonucleases. *Biochemistry (Moscow, Ruus. Fed.) 69*, 587−601.

(2) Lazarus, R. A. (2002) Human Deoxyribonucleases. In *Wiley Encyclopedia of Molecular Medicine* (Creighton, T. E., Ed.) pp 1025−1028, John Wiley and Sons, New York.

(3) Horton, N. C. (2008) DNA Nucleases. In *Protein-nucleic acid interactions: Structural biology* (Rice, P. A., and Correll, C. C., Eds.) pp 333−363, Royal Society of Chemistry Publishing, Cambridge, U.K.

(4) Yang, W. (2011) Nucleases: Diversity of structure, function and mechanism. *Q. Rev. Biophys. 44*, 1−93.

(5) Fuchs, H. J., Borowitz, D. S., Christiansen, D. H., Morris, E. M., Nash, M. L., Ramsey, B. W., Rosenstein, B. J., Smith, A. L., and Wohl, M. E. (1994) Effect of aerosolized recombinant human DNase on exacerbations of respiratory symptoms and on pulmonary function in patients with cystic fibrosis. *N. Engl. J. Med. 331*, 637−642.

(6) Suri, R. (2005) The use of human deoxyribonuclease (rhDNase) in the management of cystic fibrosis. *BioDrugs 19*, 135−144.

(7) Lazarus, R. A., and Wagener, J. S. (2007) Recombinant Human Deoxyribonuclease I. In *Pharmaceutical Biotechnology: Fundamental and Applications* (Crommelin, D. J. A., Sindelar, R. D., and Meibohm, B., Eds.) 3rd ed., pp 387−398, Informa Healthcare, New York.

(8) Shak, S., Capon, D. J., Hellmiss, R., Marsters, S. A., and Baker, C. L. (1990) Recombinant human DNase I reduces the viscosity of cystic fibrosis sputum. *Proc. Natl. Acad. Sci. U.S.A. 87*, 9188−9192.

(9) Shak, S. (1995) Aerosolized recombinant human DNase I for the treatment of cystic fibrosis. *Chest 107*, 65S−70S.

(10) Davis, J. C., Jr., Manzi, S., Yarboro, C., Rairie, J., McInnes, I., Averthelyi, D., Sinicropi, D., Hale, V. G., Balow, J., Austin, H., Boumpas, D. T., and Klippel, J. H. (1999) Recombinant human Dnase I (rhDNase) in patients with lupus nephritis. *Lupus 8*, 68−76.

(11) Martinez Valle, F., Balada, E., Ordi-Ros, J., and Vilardell-Tarres, M. (2008) DNase 1 and systemic lupus erythematosus. *Autoimmun. Rev. 7*, 359−363.

(12) Riethmueller, J., Borth-Bruhns, T., Kumpf, M., Vonthein, R., Wiskirchen, J., Stern, M., Hofbeck, M., and Baden, W. (2006) Recombinant human deoxyribonuclease shortens ventilation time in young, mechanically ventilated children. *Pediatric Pulmonology 41*, 61−66.

(13) Hendriks, T., de Hoog, M., Lequin, M. H., Devos, A. S., and Merkus, P. J. (2005) DNase and atelectasis in non-cystic fibrosis pediatric patients. *Critical Care 9*, R351−R356.
(14) Cimmino, M., Nardone, M., Cavaliere, M., Plantulli, A., Sepe, A., Esposito, V., Mazzarella, G., and Raia, V. (2005) Dornase alfa as postoperative therapy in cystic fibrosis sinonasal disease. *Arch. Otolaryngol., Head Neck Surg. 131*, 1097−1101.
(15) Rahman, N. M., Maskell, N. A., West, A., Teoh, R., Arnold, A., Mackinlay, C., Peckham, D., Davies, C. W., Ali, N., Kinnear, W., Bentley, A., Kahan, B. C., Wrightson, J. M., Davies, H. E., Hooper, C. E., Lee, Y. C., Hedley, E. L., Crosthwaite, N., Choo, L., Helm, E. J., Gleeson, F. V., Nunn, A. J., and Davies, R. J. (2011) Intrapleural use of tissue plasminogen activator and DNase in pleural infection. *N. Engl. J. Med. 365*, 518−526.
(16) Simpson, G., Roomes, D., and Reeves, B. (2003) Successful treatment of empyema thoracis with human recombinant deoxyribonuclease. *Thorax 58*, 365−366.
(17) Lazarides, E., and Lindberg, U. (1974) Actin is the naturally occurring inhibitor of deoxyribonuclease I. *Proc. Natl. Acad. Sci. U.S.A. 71*, 4742−4746.
(18) Mannherz, H. G., Goody, R. S., Konrad, M., and Nowak, E. (1980) The interaction of bovine pancreatic deoxyribonuclease I and skeletal muscle actin. *Eur. J. Biochem. 104*, 367−379.
(19) Junowicz, E., and Spencer, J. H. (1973) Studies on bovine pancreatic deoxyribonuclease A. II. The effect of different bivalent metals on the specificity of degradation of DNA. *Biochim. Biophys. Acta 312*, 85−102.
(20) Chen, W. J., and Liao, T. H. (2006) Structure and function of bovine pancreatic deoxyribonuclease I. *Protein Pept. Lett. 13*, 447−453.
(21) Moore, S. (1981) Pancreatic DNase. In *The Enzymes* (Boyer, P. D., Ed.) 3rd ed., pp 281−296, Academic Press, New York.
(22) Melgar, E., and Goldthwait, D. A. (1968) Deoxyribonucleic acid nucleases. II. The effects of metals on the mechanism of action of deoxyribonuclease I. *J. Biol. Chem. 243*, 4409−4416.
(23) Price, P. A. (1975) The essential role of Ca^{2+} in the activity of bovine pancreatic deoxyribonuclease. *J. Biol. Chem. 250*, 1981−1986.
(24) Campbell, V. W., and Jackson, D. A. (1980) The effect of divalent cations on the mode of action of DNase I. The initial reaction products produced from covalently closed circular DNA. *J. Biol. Chem. 255*, 3726−3735.
(25) Sanders, N. N., Franckx, H., De Boeck, K., Haustraete, J., De Smedt, S. C., and Demeester, J. (2006) Role of magnesium in the failure of rhDNase therapy in patients with cystic fibrosis. *Thorax 61*, 962−968.
(26) Lahm, A., and Suck, D. (1991) DNase I-induced DNA conformation. 2 Å structure of a DNase I-octamer complex. *J. Mol. Biol. 222*, 645−667.
(27) Weston, S. A., Lahm, A., and Suck, D. (1992) X-ray structure of the DNase I-d$(GGTATACC)_2$ complex at 2.3 Å resolution. *J. Mol. Biol. 226*, 1237−1256.
(28) Suck, D., Lahm, A., and Oefner, C. (1988) Structure refined to 2 Å of a nicked DNA octanucleotide complex with DNase I. *Nature 332*, 464−468.
(29) Oefner, C., and Suck, D. (1986) Crystallographic refinement and structure of DNase I at 2 Å resolution. *J. Mol. Biol. 192*, 605−632.
(30) Ulmer, J. S., Herzka, A., Toy, K. J., Baker, D. L., Dodge, A. H., Sinicropi, D., Shak, S., and Lazarus, R. A. (1996) Engineering actin-resistant human DNase I for treatment of cystic fibrosis. *Proc. Natl. Acad. Sci. U.S.A. 93*, 8225−8229.
(31) Pan, C. Q., and Lazarus, R. A. (1997) Engineering hyperactive variants of human deoxyribonuclease I by altering its functional mechanism. *Biochemistry 36*, 6624−6632.
(32) Pan, C. Q., Dodge, T. H., Baker, D. L., Prince, W. S., Sinicropi, D. V., and Lazarus, R. A. (1998) Improved potency of hyperactive and actin-resistant human DNase I variants for treatment of cystic fibrosis and systemic lupus erythematosus. *J. Biol. Chem. 273*, 18374−18381.
(33) Mol, C. D., Izumi, T., Mitra, S., and Tainer, J. A. (2000) DNA-bound structures and mutants reveal abasic DNA binding by APE1 and DNA repair coordination [corrected]. *Nature 403*, 451−456.
(34) Dlakic, M. (2000) Functionally unrelated signalling proteins contain a fold similar to Mg^{2+}-dependent endonucleases. *Trends Biochem. Sci. 25*, 272−273.
(35) Carpenter, E. P., Corbett, A., Thomson, H., Adacha, J., Jensen, K., Bergeron, J., Kasampalidis, I., Exley, R., Winterbotham, M., Tang, C., Baldwin, G. S., and Freemont, P. (2007) AP endonuclease paralogues with distinct activities in DNA repair and bacterial pathogenesis. *EMBO J. 26*, 1363−1372.
(36) Ago, H., Oda, M., Takahashi, M., Tsuge, H., Ochi, S., Katunuma, N., Miyano, M., and Sakurai, J. (2006) Structural basis of the sphingomyelin phosphodiesterase activity in neutral sphingomyelinase from *Bacillus cereus*. *J. Biol. Chem. 281*, 16157−16167.
(37) Wang, H., Morita, M., Yang, X., Suzuki, T., Yang, W., Wang, J., Ito, K., Wang, Q., Zhao, C., Bartlam, M., Yamamoto, T., and Rao, Z. (2010) Crystal structure of the human CNOT6L nuclease domain reveals strict poly(A) substrate specificity. *EMBO J. 29*, 2566−2576.
(38) Sulzenbacher, G., Gruez, A., Roig-Zamboni, V., Spinelli, S., Valencia, C., Pagot, F., Vincentelli, R., Bignon, C., Salomoni, A., Grisel, S., Maurin, D., Huyghe, C., Johansson, K., Grassick, A., Roussel, A., Bourne, Y., Perrier, S., Miallau, L., Cantau, P., Blanc, E., Genevois, M., Grossi, A., Zenatti, A., Campanacci, V., and Cambillau, C. (2002) A medium-throughput crystallization approach. *Acta Crystallogr. D58*, 2109−2115.
(39) Kabsch, W. (1993) Automatic processing of rotation diffraction data from crystals of initially unknown symmetry and cell constants. *J. Appl. Crystallogr. 26*, 795−800.
(40) Brünger, A. T. (1992) The free R value: A novel statistical quantity for assessing the accuracy of crystal structures. *Nature 355*, 472−474.
(41) Collaborative Computational Project, Number 4 (1994) The CCP4 suite: Programs for protein crystallography. *Acta Crystallogr. D50*, 760−763.
(42) Murshudov, G. N., Vagin, A. A., and Dodson, E. J. (1997) Refinement of macromolecular structures by the maximum-likelihood method. *Acta Crystallogr. D53*, 240−255.
(43) Emsley, P., and Cowtan, K. (2004) Coot: Model-building tools for molecular graphics. *Acta Crystallogr. D60*, 2126−2132.
(44) Holm, L., and Rosenstrom, P. (2010) Dali server: Conservation mapping in 3D. *Nucleic Acids Res. 38* (Suppl.), W545−W549.
(45) Murzin, A. G., Brenner, S. E., Hubbard, T., and Chothia, C. (1995) SCOP: A structural classification of proteins database for the investigation of sequences and structures. *J. Mol. Biol. 247*, 536−540.
(46) *The PyMOL Molecular Graphics System*, version 1.3r1 (2010) Schrodinger, LLC, New York.
(47) Suck, D. (1994) DNA recognition by DNase I. *J. Mol. Recognit. 7*, 65−70.
(48) Suck, D., Oefner, C., and Kabsch, W. (1984) Three-dimensional structure of bovine pancreatic DNase I at 2.5 Å resolution. *EMBO J. 3*, 2423−2430.
(49) Chereau, D., Kerff, F., Graceffa, P., Grabarek, Z., Langsetmo, K., and Dominguez, R. (2005) Actin-bound structures of Wiskott-Aldrich syndrome protein (WASP)-homology domain 2 and the implications for filament assembly. *Proc. Natl. Acad. Sci. U.S.A. 102*, 16644−16649.
(50) Doherty, A. J., Worrall, A. F., and Connolly, B. A. (1995) The roles of arginine 41 and tyrosine 76 in the coupling of DNA recognition to phosphodiester bond cleavage by DNase I: A study using site-directed mutagenesis. *J. Mol. Biol. 251*, 366−377.
(51) Kabsch, W., Mannherz, H. G., Suck, D., Pai, E. F., and Holmes, K. C. (1990) Atomic structure of the actin:DNase I complex. *Nature 347*, 37−44.
(52) Wolf, E., Frenz, J., and Suck, D. (1995) Structure of human pancreatic DNase I at 2.2 Å resolution. *Protein Eng. 8* (Suppl.), 79.
(53) Harding, M. M. (1999) The geometry of metal-ligand interactions relevant to proteins. *Acta Crystallogr. D55*, 1432−1443.
(54) Jones, S. J., Worrall, A. F., and Connolly, B. A. (1996) Site-directed mutagenesis of the catalytic residues of bovine pancreatic deoxyribonuclease I. *J. Mol. Biol. 264*, 1154−1163.
(55) Pan, C. Q., and Lazarus, R. A. (1999) Ca^{2+}-dependent activity of human DNase I and its hyperactive variants. *Protein Sci. 8*, 1780−1788.

(56) Evans, S. J., Shipstone, E. J., Maughan, W. N., and Connolly, B. A. (1999) Site-directed mutagenesis of phosphate-contacting amino acids of bovine pancreatic deoxyribonuclease I. *Biochemistry 38*, 3902−3909.
(57) Chen, C. Y., Lu, S. C., and Liao, T. H. (2002) The distinctive functions of the two structural calcium atoms in bovine pancreatic deoxyribonuclease. *Protein Sci. 11*, 659−668.
(58) Gueroult, M., Picot, D., Abi-Ghanem, J., Hartmann, B., and Baaden, M. (2010) How cations can assist DNase I in DNA binding and hydrolysis. *PLoS Comput. Biol. 6*, e1001000.
(59) Beernink, P. T., Segelke, B. W., Hadi, M. Z., Erzberger, J. P., Wilson, D. M., III, and Rupp, B. (2001) Two divalent metal ions in the active site of a new crystal form of human apurinic/apyrimidinic endonuclease, Ape1: Implications for the catalytic mechanism. *J. Mol. Biol. 307*, 1023−1034.
(60) Gorman, M. A., Morera, S., Rothwell, D. G., de La Fortelle, E., Mol, C. D., Tainer, J. A., Hickson, I. D., and Freemont, P. S. (1997) The crystal structure of the human DNA repair endonuclease HAP1 suggests the recognition of extra-helical deoxyribose at DNA abasic sites. *EMBO J. 16*, 6548−6558.
(61) Lowry, D. F., Hoyt, D. W., Khazi, F. A., Bagu, J., Lindsey, A. G., and Wilson, D. M., III (2003) Investigation of the role of the histidine-aspartate pair in the human exonuclease III-like abasic endonuclease, Ape1. *J. Mol. Biol. 329*, 311−322.
(62) Chen, W. J., Lai, P. J., Lai, Y. S., Huang, P. T., Lin, C. C., and Liao, T. H. (2007) Probing the catalytic mechanism of bovine pancreatic deoxyribonuclease I by chemical rescue. *Biochem. Biophys. Res. Commun. 352*, 689−696.